Applied Water Science (2024) 14:205
https://doi.org/10.1007/s13201-024-02258-4

ORIGINAL ARTICLE

A promising sustainable green nanosilver formula for *p*-nitrophenol and methylene blue remediation from wastewater

Ayman H. Mansee[1] · **Amal M. Ebrahim**[2] · **Essam A. Koreish**[2]

Received: 28 November 2023 / Accepted: 30 July 2024 / Published online: 20 August 2024

Abstract

In an attempt to create wastewater treatment "green" techniques that are both economically feasible and sustainable without using any dangerous chemicals, barley grain (*Hordeum vulgare* L.) water extract was used to phyto-synthesize silver nanoparticles (Ag°). Barley grains served as a natural reductant and stabilizer at the same time. The role of different synthesis conditions and their effect on the efficiency of the green synthesis process were studied and confirmed with characterization using several techniques (UV–vis, SEM, EDX, sizing distribution, and FTIR). The Ag°9 formula catalytic reduction was inspected against *p*-nitrophenol (PNP) and methylene blue (MB) as a model of nitroaromatic components and dyes, respectively. The removal studies were conducted using the target pollutants in a single or mixed liquid state. Remarkably, the Ag°9 particle size was around 20 nm, and its final concentration in the current formula was 2.2×10^{-7} mol L^{-1}. The adsorption mechanism of the PNP and MB was pseudo-second order. The good fit with the pseudo-second-order kinetic model suggests that chemisorption occurs in the sorption process. The formula catalytic activity to remove PNP and MB was 99 and 66% at levels 60 and 500 µL from the Ag°9 formula, respectively, within less than 5 min.

Keywords Green silver nanoparticles · *Hordeum vulgare* L. · Catalytic activity · Wastewater treatment · *p*-nitrophenol · Methylene blue

Introduction

The management of freshwater resources is one of the most urgent issues facing the globe today, as two-thirds of its population is predicted to experience moderate to severe water stress by 2025 (Zhang and Shen 2017). Moreover, Mashkoor et al. (2020) claim that industry, household consumption, and agriculture use nearly one-third of the world's renewable freshwater supply, and that most of these activities contaminate water with various man-made substances like pesticides, fertilizers, dyes, and heavy metals.

The US Environmental Protection Agency (US-EPA) has identified 129 organic compounds as potentially carcinogenic pollutants, *p*-nitrophenol (PNP) being one of them. PNP is among the worst organic pollutants that come from agriculture and industrial processes. Because it dissolves easily in water, it is found in large quantities in soil, air, and industrial effluents (Rajegaonkar et al. 2018; Zhang et al. 2022; Mansee et al. 2023). Also, methylene blue (MB) is a dye with several applications, such as aquaculture, antimalarial drugs, chemotherapy, and medicine. It is widely used in most industries that pollute our atmosphere. These compounds are generally stable to light, oxidizing agents and are resistant to aerobic digestion (Rajegaonkar et al. 2018; Rahmi et al. 2019).

Many physical, chemical, and biological remediation techniques have been modified to achieve wastewater reuse in agriculture and industry safely and without endangering the environment (Mansee et al. 2023; Abdelgawad et al. 2022; Khan et al. 2022; Mansee et al. 2020; Rahmi et al. 2019). Among such techniques is nanotechnology, which has numerous uses in the environment, including remediation, monitoring, detection, and pollution prevention (Ganie et al.

✉ Ayman H. Mansee
amansee@alexu.edu.eg

Amal M. Ebrahim
amal.mohammed@alexu.edu.eg

Essam A. Koreish
Essam.quraish@alexu.edu.eg

[1] Department of Pesticide Chemistry and Technology, Faculty of Agriculture, Alexandria University, Alexandria, Egypt

[2] Department of Soil and Water Science, Faculty of Agriculture, Alexandria University, Alexandria, Egypt

2021). Metal nanoparticles have been synthesized using a variety of chemical, physical, and biological techniques; unfortunately, these methods are very expensive and may involve dangerous chemicals for synthesis.

Green synthesis is similar to chemical reduction, but in this method, expensive chemical reducing agents are replaced by different plant extracts for the synthesis of metal or metal oxide NPs (Chand et al. 2020). Behravan et al. (2019) and Iravani et al. (2011) clarified that the primary issues encountered are: nanoparticle aggregation, stability, control over crystal development, shape, size, and size distribution. It has been demonstrated that plants create metal nanoparticles faster and more steadily than other creatures do. Plant extracts are also undoubtedly preferable to plant biomass or live plants when it comes to using a simple, safe, and green method for the industrial scale-up and manufacturing of well-dispersed metal nanoparticles. While chemical reduction and the green synthesis of nanoparticles are comparable processes, the latter uses extracts of certain natural bio-products in place of the former (Khaturia et al. 2020).

Haldar et al. (2022) **concluded that** the biosynthesis method depends on the presence of phytochemicals like alkaloids, phenols, citric acid, polyphenols, terpenes, ascorbic acid, flavonoids, and other components in certain plant parts (stems, roots, buds, leaves, seeds, and rhizomes), which play a crucial role in being reducing agents. Also, Abada et al. (2023) added that plant extracts are able to provide several phytochemicals like proteins, amino acids, carbohydrates, saponins, flavonoids, chromones, steroids, saturated and unsaturated fatty acids, terpenoids, and phytol that have a great influence on physical and organic chemical fundamentals, which play an essential role in improving reduction size, rate, and stabilization.

In this context, the study delves into synthesizing silver NPs using barley grains. The most important thing about barley grains is that they contain antioxidant components such as 2″(3″)-o-glycosylisovitexin. Barley grains are readily available on a large scale, making them a cost-effective resource for nanoparticle production. Their abundance ensures a consistent and reliable supply, reducing dependency on fluctuating market conditions or seasonal variations. Moreover, the cultivation of barley is relatively sustainable, requiring minimal inputs such as water and fertilizers compared to other crops, thus aligning with eco-friendly practices (Singh et al. 2024; Duh et al. 2001; Din et al. 2020).

Recently, silver nanoparticles (AgNPs) have greatly focused the researcher's attention because of their important application as antimicrobial, catalytic, textile fabrics, and plastics to eliminate microorganisms (Fouad et al. 2019; Kalpana et al. 2019). As mention by Rajegaonkar et al. (2018), green silver nanoparticles (AgNPs) are one type of metal nanoparticle that is being extensively studied. They further state that AgNPs use the electron relay effect between donor and acceptor molecules to function as a redox catalyst in the degradation of organic contaminants. Karki et al. (2018) and Liao et al. (2019a) reported that green silver nanoparticles (AgNPs) are one type of noble metal nanoparticle that is being extensively studied. They further state that AgNPs have advantages over other noble nanoparticles in the catalytic reduction of water pollutants, and it was classified as an attractive and ideal catalyst material. Also, they summarized the most important advantages of AgNPs in the following points: (1) The catalytic activity of AgNPs is easily tuned using the particle size, shape, and temperature; (2) AgNPs catalysts are active under mild conditions or even ambient temperature, and (3) AgNPs catalysts are particularly suitable for practical applications due to their relatively low prices, generally less than 1/50 of that of Au or Pt and about 1/25 of that of Pd; and (4) AgNPs catalysts are endowed with high application value owing to their relatively low toxicity. They also added that Ag-based nanocomposites are also outstanding catalysts for many catalytic reduction reactions, such as aqueous phase organic pollutants' reduction, nitrogen oxide (NOx) reduction, and acetylene reduction, due to their relatively low cost and high catalytic activity.

Although 4-nitrophenol (4-NP) is a highly toxic compound (Bilal et al. 2021), its reduction product, 4-aminophenol (4-AP), is considered less toxic and has many beneficial uses, including corrosion inhibition, anticorrosion lubrication, drying agents, and photographic development (Saran et al. 2018). Therefore, one of the most important objectives of this study was to present an environmentally friendly, economical, and simple model that has the ability to reduce 4-NP to 4-AP. According to Liao et al. (2019b), the most commonly used but highly efficient strategy for the catalytic reduction of 4-NP to 4-AP is effectively utilizing metal NPs. Among these metal NPs catalysts, AgNPs have been widely used as one of the most effective catalysts. The expected reaction pathway for the catalytic reduction of 4-NP to 4-AP through Ag-based NPs catalysts with $NaBH_4$ can be summarized as follows: $NaBH_4$ is first converted to $B(OH)^{4-}$ and active hydrogen species via hydrolysis reactions. The generated active hydrogen species and 4-NP are then adsorbed on AgNPs surface. Next, the active hydrogen species adsorbed on the surface of AgNPs. Next, the active hydrogen species adsorbed on AgNPs surface will further react with 4-NP to produce 4-AP. Notably, all reduction reactions are carried out on the surface of Ag NPs with an adsorption–desorption equilibrium.

Liao et al. (2016) studied the catalytic activities of polystyrene-methyl acrylic acid/silver (PSMAA/Ag) nanocomposite. They found that PSMAA/Ag nanocomposite exhibits high catalytic activity for the reduction of 4-nitrophenol to 4-aminophenol. Liu et al. (2023a) synthesized small-sized

silver (Ag) nanoparticles (NPs) on sepia eumelanin (SE) and artificial allomelanin (AMNP) and used it to remove PNP and MB. Zhu et al. (2023) prepared $ZnFe_2O_4$ (ZFO) with Ag-doping. They found that the prepared MoS_2/Ag-ZFO (T) has excellent photocatalytic performance under real environment water. Liu et al. (2023b) used ultrafine Ag nanoparticles (average size of approximately 4.37 nm) decorated on the surface of pure silicon zeolite nanoparticles (PSZN) as a low-cost and environmentally friendly in situ reduction strategy. The prepared Ag/PSZN nanocomposites showed ultrahigh catalytic activity for the reduction of 4-nitrophenol and methylene blue. Moreover, it showed outstanding recyclability of 93% and 86% removal of 4-NP and MB, respectively, after 10 cycle reactions, and stability after 300 days of storage at room temperature. Ouyang et al. (2024) introduced an efficient catalyst, composed of silver-decorated polydopamine coatings on pure silicon zeolite (PSZN/PDA/Ag), capable of removing methylene blue (MB) and 4-nitrophenol (4-NP) in water effectively. Chand et al. (2020) used extracts of different plants (onion, tomato, and acacia catechu alone) to create silver nanoparticles in an environmentally friendly manner, and they used the produced AgNPs as catalysts to remove methyl orange, methyl red, and Congo red. Another study looked at how silver nanoparticles made via microbiologic synthesis catalytically reduced p-nitrophenol (PNP) and methylene blue (MB), and they came to the conclusion that extracellular AgNPs displayed outstanding catalytic activity for the reduction of PNP and MB (Rajegaonkar et al. 2018). The current study aimed to develop a safe, economical, efficient, and environmentally friendly synthetized Ag° formula by using the water extract of barley grain ($BG_{ex.}$) as a naturally reducing, stabilizing, and capping agent for nanosilver green synthesis. Also, find the ideal operating parameters for eliminating PNP and MB from artificially contaminated water.

Material and methods

Green synthesis process

Extracting the reducing agent from barley grains (BG_{ex})

Fresh barley grains were obtained from the local grain market to extract the reducing and capping agents without solvents. The water extraction process was conducted according to Duh et al. (2001) and Chand et al. (2020) with some modifications. The collected grains were thoroughly washed with distilled water, followed by deionized water, to remove dust particles. Then, a series of barley extract concentrations (10, 20, and 30%, w/v) was prepared by boiling the grains with deionized water at 80 °C for 20 min (Table 1). Finally, the solution was let for coaling and then filtered.

Phyto-synthesis of silver nanoparticles (Ag°)

The Ag° phyto-synthesis process was carried out according to Shimoga et al. (2020a, 2020b). In this section, different operating factors were studied in order to optimize the reduction of Ag^{++} to Ag° using the previously prepared barley water extract, as illustrated in Table 1. These factors were: $AgNO_3/BG_{ex.}$ ratios (1:1, 1:2, and 1:3), level of BG_{ex} pH (natural and 12), concentration of BG_{ex} (10, 20, and 30%), and $AgNO_3$ final concentration (2 and 4 mM). Generally, all the phytosynthesis steps were carried out using deionized water under the following conditions: shaking at 90 °C for 20 min in a dark environment. Visual observation of the solution's color change from yellow to brownish-yellow to deep brown was the primary method used to monitor the reduction process. The produced Ag° particles were scanned by UV–visible Spectrophotometer Alpha 1502 (Laxco, Inc., Bothell, WA 98021, USA) at an interval of 50 nm between 250 and 750 nm to confirm the reduction process. From the UV–vis spectrum data, the Ag°9 formula was selected for further investigation without any purification process.

Characterization of the Ag°9 formula

Standard methods for studying nanomaterials were used to recognize the main characteristic of the Ag°9 formula (Chand et al. 2020). The surface morphology and element contents of the Ag°9 formula were examined using scanning electron microscopy (SEM) in combination with an energy-dispersive X-ray (EDX, MODEL JSM-IT200). The chemical constituents responsible for the reduction of silver ions and the capping agent of silver nanoparticles were studied using FTIR spectroscopy. A small amount of Ag°9 formula was crushed with KBr powder, and the FTIR analysis was measured in the 4000–500 cm^{-1} region using a PerkinElmer spectrum analyzer. The Malvern Zeta Sizer was utilized to

Table 1 Summary of the optimal green synthesis conditions

Phyto-synthesis parameter	Ag°1	Ag°2	Ag°3	Ag°4	Ag°5	Ag°6	Ag°7	Ag°8	Ag°9
Extract pre-concentration (%)	10	10	10	10	10	10	10	20	**30**
pH level	7	7	7	12	12	12	12	12	**12**
$AgNO_3$: extract ratio (v:v)	1:1	1:2	1:3	1:1	1:2	1:3	1:3	1:3	**1:3**
$AgNO_3$ final concentration (mM)	2	2	2	2	2	2	4	4	**4**

examine the size and dispersion of nanoparticles in aqueous media at a temperature of 25 °C.

Investigation of the optimum operating conditions through batch sorption experiments

A series of batch experiments (Ag°9 dose, contact time, and the initial concentration) of different target pollutants were conducted to evaluate the catalytic potential of the Ag°9 formula for removing *p*-nitrophenol (PNP), methylene blue (MB), and their mixture from synthetically contaminated water.

The pH point of zero charge (pH_{pzc})

pH_{pzc} for the Ag°9 formula was determined according to Singh et al. (2023). Two milliliters of the Ag°9 formula were added to 20 ml of 0.1 mM NaCl with a pre-adjusted pH range of 2 to 11 using 0.1 M NaOH or HCl. After 24 h of shaking, the final pH values were measured. Plotting the difference between the initial and final pH values versus the initial pH values was done. As shown in Fig. 3, the pH_{pzc} was determined from the pH axis intersection point.

Sorbent dose

To study the impact of Ag°9 dosage on the removal of PNP, MB, and their mixture, various sorbent doses of 20, 40, 60, 120, 240, and 500 µl mL^{-1} were tested at normal pH and room temperature.

For each case, a water solution of the 100 µg mL^{-1} tested pollutants was scanned at its specific λ_{max} (PNP, 365–500 nm; MB, 550–700 nm; and PNP-MB mixture, 365–700 nm) using a UV–vis spectrophotometer; the control sample was distilled water. In the case of PNP samples, 300 µl mL^{-1} of $NaBH_4$ (0.5 mM) was added. Then, various Ag°9 doses (20, 40, 60, 120, 240, and 500 µl mL^{-1}) were added to the previous samples. After 60 min of shaking, the reaction progress was recorded using a UV–visible spectrophotometer, and then, the removal efficiency (R, %) was calculated as mentioned in Eq. 1. (Albukharia et al. 2019).

$$R(\%) = \frac{C_i - C_t}{C_i} \times 100 \quad (1)$$

where C_i and C_t are the initial and final concentrations of the target pollutant (µg mL^{-1}), respectively.

Initial concentration and sorption kinetics

The influences of contact time (5 to 240 min) and the initial concentration of the target pollutant on the Ag°9 sorption capacity were examined using different initial concentrations of PNP (2–500 µg ml^{-1}) and MB (10–100 µg ml^{-1}) while conserving other experimental conditions as illustrated in the sorbent dose section. The removal efficiency (R, %) and amount of sorbed pollutant (qe, mg g^{-1}) were monitored using a UV–visible spectrophotometer and calculated as mentioned in Eqs. 1 and 2, respectively (Mansee et al. 2023).

$$q_e = \frac{V(C_0 - C_e)}{m} \quad (2)$$

where q_e is the amount of sorbed pollutant per gram of Ag°, V refers to the volume of solution,, C_0 and C_e are the initial and final pollutant concentrations, and m is the weight of Ag°.

PNP-MB mixture

In this section, an artificially contaminated water sample contains a mixture of PNP-MB at 100 µg mL^{-1} for each of them and 300 µl mL^{-1} of $NaBH_4$ (0.5 mM) was prepared. The samples were scanned (365 to 700 nm) before and after 5 min of incubation with 500 µg mL^{-1} Ag°9, and the effect of temperatures (5 to 45 °C) was also studied. The removal percentage was calculated using the previously mentioned in Eq. 1. Also, FTIR analysis was carried out on Ag°9 after the sorption process to test the effect of interaction between the PNP-MB mixture and Ag°9 on the functional groups, as mentioned in the characterization section.

Results and discussion

Spectroscopic measurements of green synthetic Ag°

To investigate the formation and stabilization of the green synthesized Ag°, UV–vis spectroscopy was utilized according to Chand et al 2020. As shown in Table 1, nine Ag° colloidal solutions were synthesized under different operating parameters. Visual inspection and the surface plasmon resonance data from the spectroscopic scan in Fig. 1a were used to assess the synthesized Ag° formulae. As per earlier research, the excitation of Ag° surface plasmon resonance, which signifies the decrease and uniform dispersion of spherical Ag° particles, is responsible for the color changes observed in Ag° colloidal solutions (Shimoga et al. 2020a, 2020b; Chartarrayawadee et al. 2020). The results of this study indicate that all Ag° colloidal solutions exhibit absorption peaks in the 400–450 nm range, confirming the effectiveness of the green synthesis method (Chand et al. 2020; Gopinath et al. 2017). Thus, the Ag°9 formula has the sharpest plasmon and more density compared to the other formulas. Hence, the Ag°9 formula was the promised one

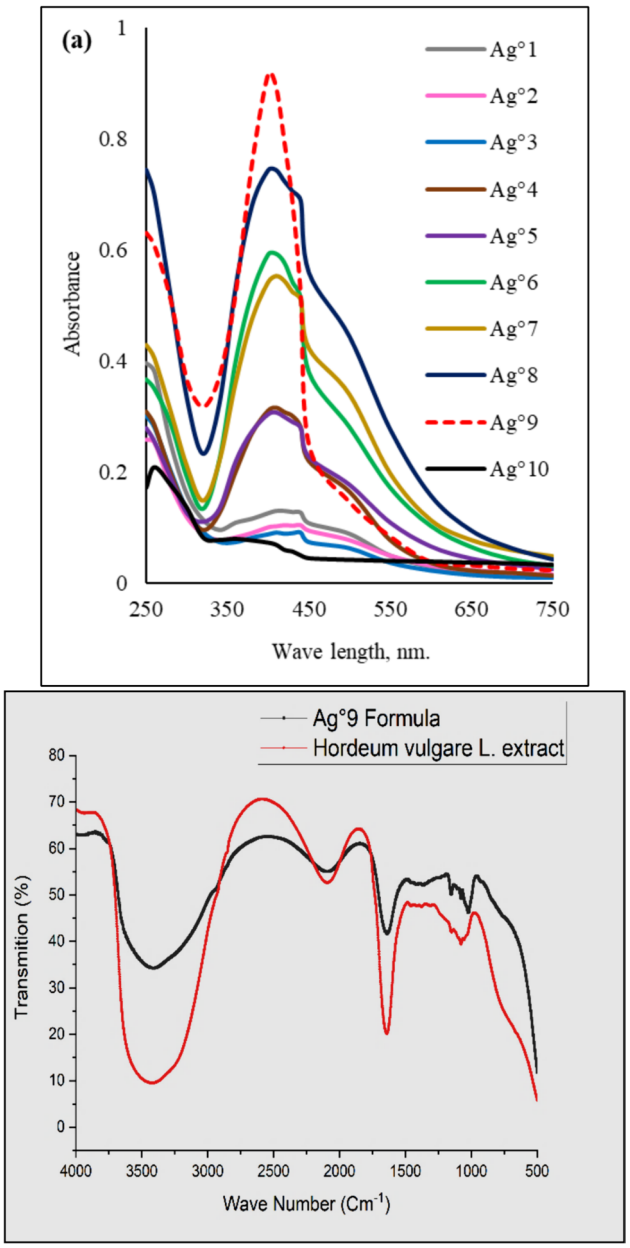

Fig. 1 Green synthesized silver nanoparticles spectroscopic measurements: **a** UV–vis spectra of nine Ag° formulas reduced by *Hordeum vulgare* L. water extract, **b** FTIR of $BG_{ex.}$ and the Ag°9 formula

and was chosen to complete further studies for its well-band development and absorbance intensity.

The potential functional groups in the biomolecules found in the plant extract that could be responsible for the reduction of Ag^{++} into Ag° were identified using FTIR analysis. Figure 1b represents the FTIR spectra of both $BG_{ex.}$ alone and the green synthesized Ag°9. According to Chartarrayawadee et al. (2020), the high similarity between the FTIR data for the plant extract ($BG_{ex.}$) and its green nanoformula (Ag°9) indicated that both tested samples had the same function groups, with a noticeable change in peak intensities and some shifting in their positions. Chand et al 2020 reported that the intense and wide peak at 3500–3200 cm^{-1} denotes the N–H, O–H, and H-bonded stretching vibrations of amide, amide groups, phenols, and alcohols, respectively. The bands appearing in the range of 1700–1600 and 1300–1000 cm^{-1} denote the C=O and C–O stretching vibrations, respectively. These biomolecules might be acting as reducing and stabilizing agents. On the other hand, Sharma et al. (2017) and Kalpana et al. (2019) concluded that the band appearing in the ranges of 1700–1600 cm^{-1} in the spectrum indicates the formation of Ag° and is capped with different biomolecules.

Scanning electron microscopy (SEM))-energy-dispersive X-ray spectrometer (EDX)

The surface morphology of the Ag°9 formula was observed using SEM at a magnification of 35,000 and a scale of 500 nm, Fig. 2a. The SEM image observed that the morphology of the Ag° 9 formula is near to being spherical in shape, and its particle sizes ranged from 5 to 24 nm. According to the EDX result, the green synthesized Ag°9 produced a strong signal at 3 keV, which confirmed the existence of Ag metal, Fig. 2b. The percentages of the elements in the Ag°9 were 22.28% C, 3.54% N, 31.98% O, 7.48% Na, 7.5% Cl, 6.49% K, and 15.73% Ag. Albukhari et al. (2019) synthesized silver nanoparticles (AgNP) using Duranta erecta leaf extract as a reducing agent. In the EDX profile, they observed a peak for silver at 3 keV, which confirmed AgNPs formation. Also, they reported that the other peaks observed were from plant-based capping agents.

Particle size distribution

For the particle size distribution, it can be observed that the Ag°9 colloidal solution has three peaks (Fig. 2c). Based on the intensity, about 70% of the particles in the current colloidal solution represent the small size of nanoparticles (27 nm), 18.8% represent the large size of Ag° (243 nm), and 10.3% of the particles represent the micro-size (5417 nm). Chartarrayawadee et al. (2020) used *Lysimachia Foenumgraecum* extract for silver nanoparticle green synthesis. When they studied the particle size distribution, they found that the nanoparticles' colloidal solution showed three different mean particle sizes presented as three picks. They concluded that these picks, due to nanoparticles, are capped by surfactants found in phytochemicals in the plant extract. Also, the mean particle should be the hydrodynamic diameters of AgNPs coated with phytochemicals (hydrodynamic radius), because phytochemical coatings on AgNPs are resulting in substantial changes in the hydrodynamic radius. This result suggests that the phytochemicals found in the

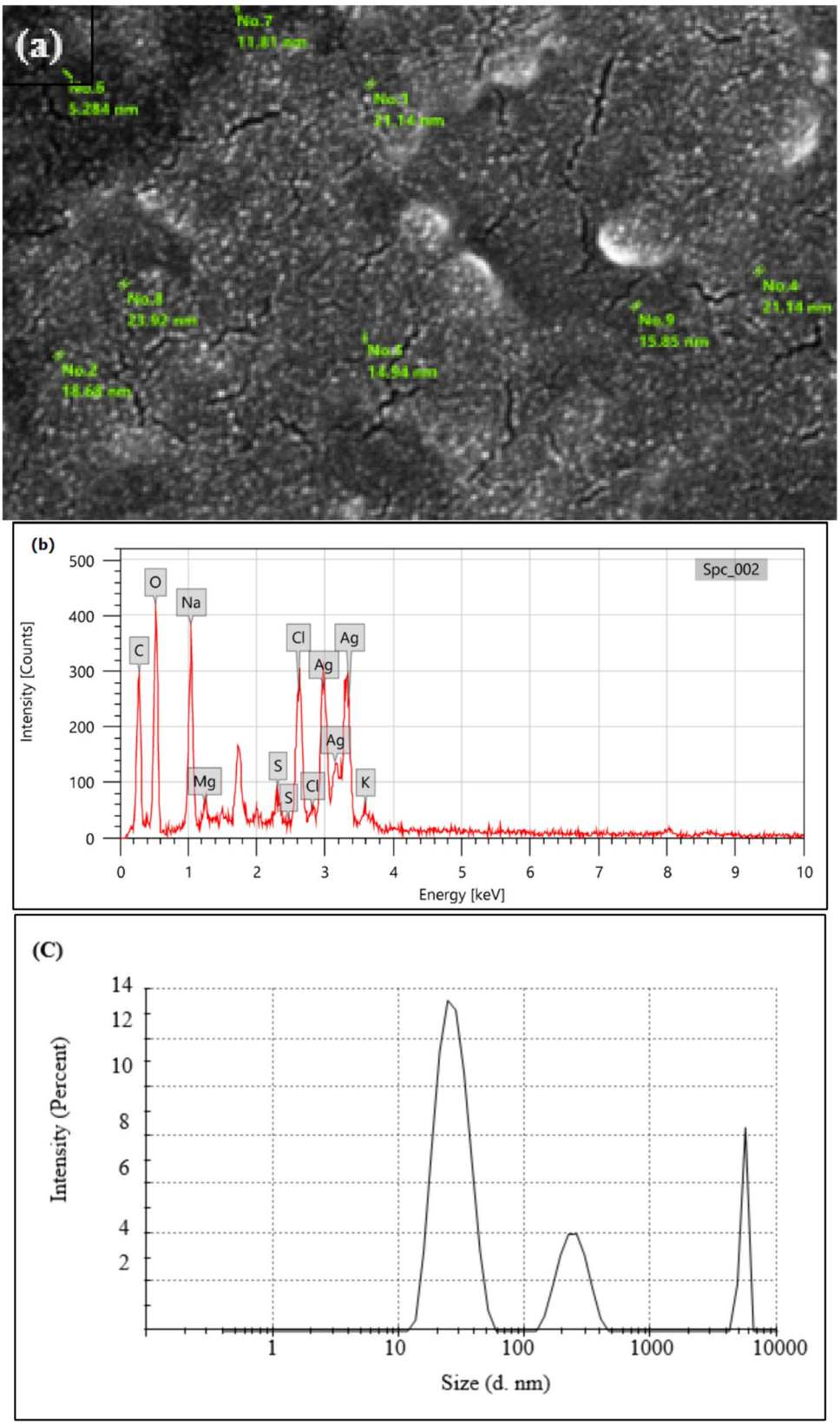

Fig. 2 Scanning electron microscopy image (**a**), EDX image (**b**), and sizing distribution (**c**) of green synthesized Ag°9 formula

plant extract are capped on AgNPs. They added that the third peak might be the size of the self-assembled surfactant aggregates or surfactant micelles that existed at high concentrations of the plant extract. The Ag° final concentration in the current formula was calculated theoretically according to Attatsi and Nsiah (2020) and the result illustrated that one litter of the Ag°9 formula contained 2.2×10^{-7} mol Ag°.

Catalytic application

In order to assess the effectiveness of the present Ag°9 formula in remediating artificially contaminated water that contains PNP, MB, or their combination, serial batch experiments were carried out in this section.

pH point of zero charge (pH_{pzc})

The degree of adsorbent surface ionization is expressed by this parameter ($\mathbf{pH_{pzc}}$). When the adsorbent surface is positively charged, it attracts anions at pH values below pH_{pzc}, while when it is negatively charged, it attracts cations at pH values above the pHpzc point (Singh et al. 2023; Azeez et al. 2018). For the current results, the pH of the Ag°9 formula was 11 and its pH_{pzc} was 9.25 (Fig. 3) which was fairly basic and able to adsorb cations. Also, the pH of all studied synthetically contaminated water was in a basic range, which was suitable to adsorb cations such as PNP (Bilal et al. 2021) and MB (Khan et al. 2022).

Adsorbent dose

The effects of the Ag°9 formula (20 to 500 µl mL^{-1}) on removing PNP, MB, or their mixtures in water samples that were intentionally contaminated were assessed. From Fig. 4a, it was observed that 100% of the PNP was removed from the tested sample due to the addition of 60 µl of Ag°9 formula, while 76% of the MB was removed using a higher

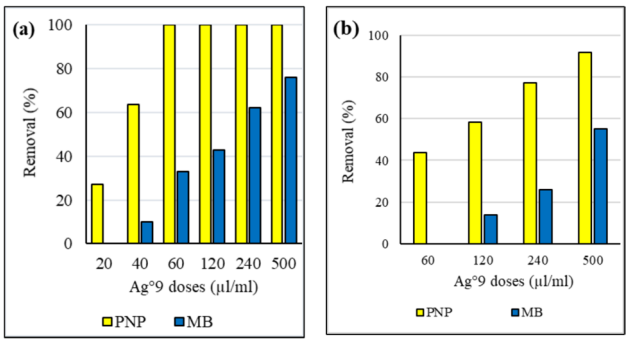

Fig. 4 Effect of Ag°9 doses on the removal efficiency (%) of PNP and MB separately (**a**), and PNP-MB mixture (**b**) from artificially contaminated water (Ag°9 dose ranged from 20 to 500 µl mL^{-1}, PNB, MB, and PNP-MB concentration = 100 µg mL^{-1}, reaction time = 60 min, the yellow bares refer to PNP removal %, while blue bares refer to MB removal %)

dosage of Agº9 (500 µl mL^{-1}). The power of the current green formula was evident in these results, even in minute quantities. While, in the case of the PNP-MB mixture, the removal percentages decreased as compared to the individual of each target (PNP or MB), Fig. 4b. Generally, the data shown in Fig. 4a, b illustrate that Agº9 has a higher ability to remove PNP than MB. It might be due to the chemical and physical properties of MB. Hence, Khan et al. (2022) cited that the MB is highly water-soluble and thus forms a stable solution with water at room temperature and is positively charged. These properties confirm the high stability and protection of MB from degradation, illustrating the need for a higher dose of Ag°9 than that of PNP.

Contact time and sorption mechanism

Depending on the results obtained from the section of adsorbent dose, the Ag°9 dosages of 60 and 500 µl mL^{-1} were selected to evaluate the role of contact time (5:240 min) on

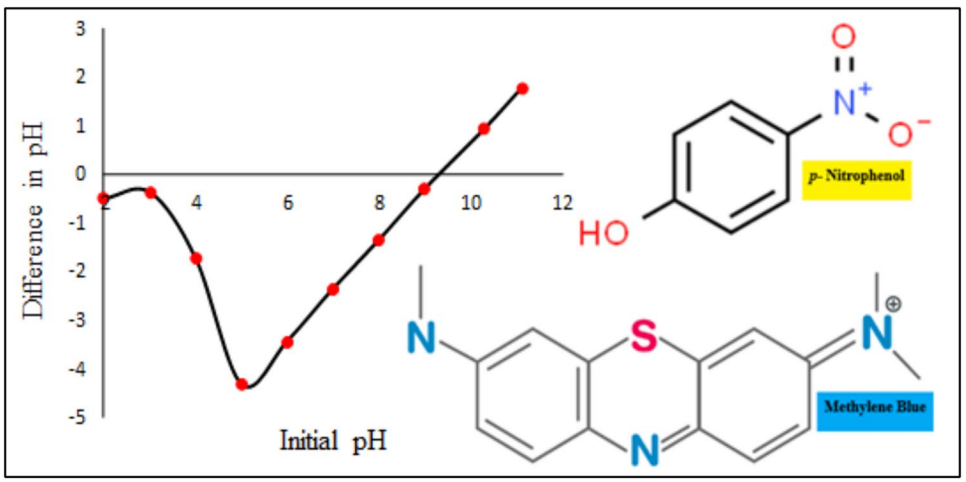

Fig. 3 pH point of zero charge of the Ag°9 formula

the removal of 100 µg ml^{-1} PNP and MB, respectively, from an artificially contaminated water sample. The recorded data represented a fast removal of either PNP or MB in less than 5 min. As a result of adding the Ag°9 formula to the target contaminated samples, the solution optical density at 400 nm for PNP (Fig. 5a) and 665 nm for MB (Fig. 5b) decreased sharply in less than 5 min of incubation. Meanwhile, new peaks appeared at 450 and 600 nm, and the increase in its optical density was parallel to the reduction observed in the intensity of the mean PNP and MB peaks, respectively. Thus, it can be observed that the tested green formula (Ag°9) was able to remove 100 µg ml^{-1} PNP and MB from artificially contaminated water in less than 5 min of incubation. Therefore, a contact time of 5 min was selected for additional investigations. A similar observation was made by Rajegaonkar et al. (2018) when they investigated the catalytic reduction of PNP and MB by microbiologically produced silver nanoparticles and found that the microbiologically produced silver nanoparticles could rapidly reduce PNP. Additionally, they saw a discernible drop in MB absorbance during the course of the incubation time.

To understand the adsorption mechanisms of the target pollutants (PNP or MB) using the Ag°9 formula, the adsorption mechanisms were investigated by applying various kinetic models, including pseudo-first order, pseudo-second order, power fraction, and Elovich (Table 2). According to the determination of coefficient values (R^2) of the tested adsorption kinetic models, the pseudo-second-order model recorded the

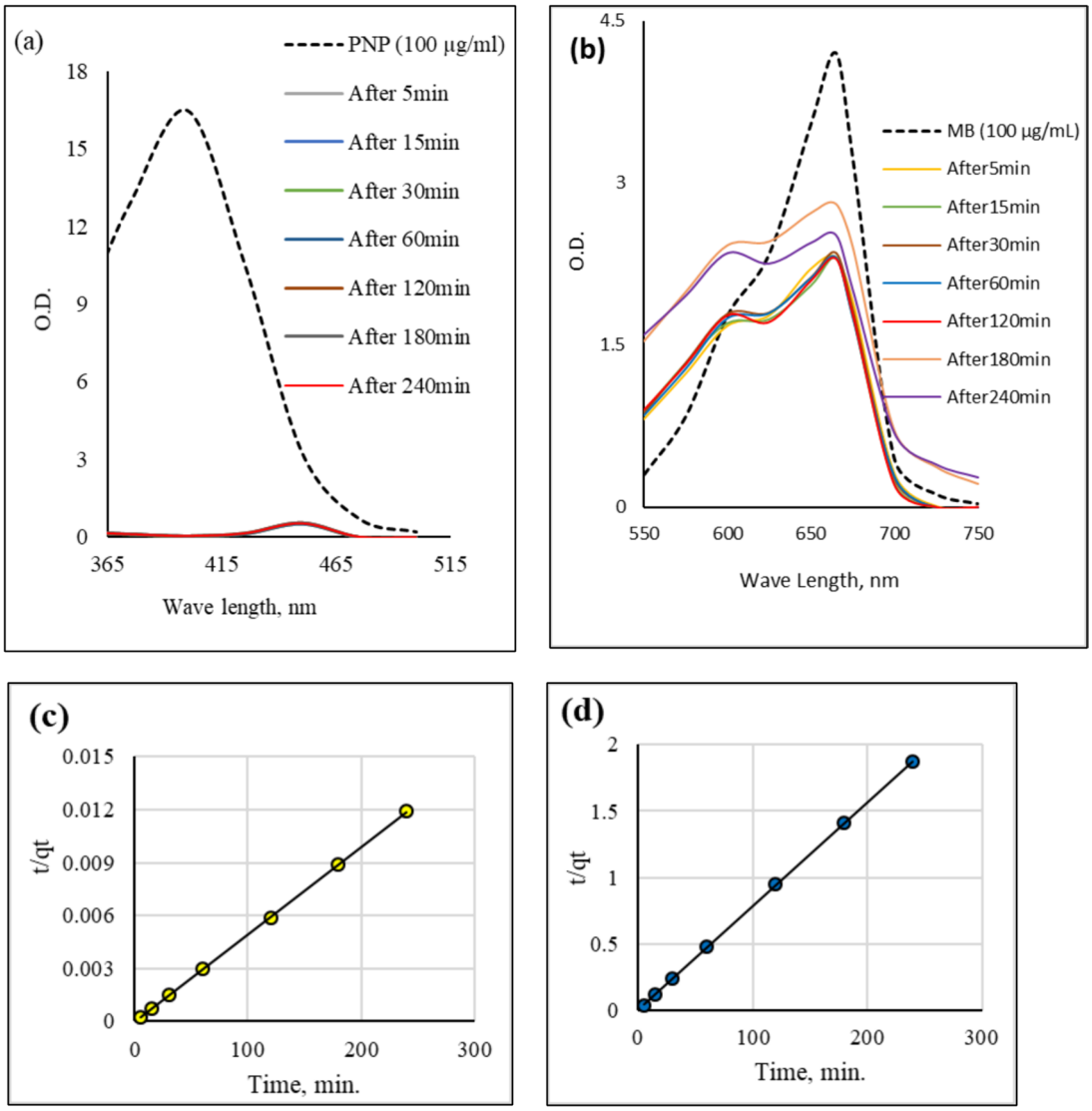

Fig. 5 UV–Vis spectra of PNP (**a**), MB (**b**) before and after treated with Ag°9, pseudo-second-order kinetic model for PNP (c) and MB(d) reduced by Ag°9 formula (contact times = 5 to 240 min, pollutant concentration = 100 µg mL^{-1}, Ag°9 dosages = 60 µl mL^{-1} for PNP samples, Ag°9 dosages = 500 µl mL^{-1} for MB samples)

Table 2 Kinetic models parameters for PNP and MB sorption by the Ag°9 formula

Kinetic parameters		Ag°9 formula	
		PNP	MB
Pseudo-first order $\ln(q_e - q_t) = \ln q_e - k_1 t$	q_e (mg g^{-1})	55.601	7.020
	K_1 (min^{-1})	0.0107	−0.014
	R^2	0.4585	0.9884
Pseudo-second order $t/q_t = \frac{1}{k_2 q_e^2} + \frac{1}{q_e t}$	q_e (mg g^{-1})	20,000	128.21
	K_2 (g mg^{-1} min^{-1})	$-9*10^{-6}$	0.01
	R^2	1.000	1.000
Power fraction $\ln q_t = \ln a + b \ln t$	a (mg g^{-1})	20,341.13	117.92
	b (min^{-1})	−0.0012	0.0149
	R^2	0.2173	0.9299
Elovich $q_t = \beta \ln(\alpha\beta) + \beta \ln t$	β (g mg^{-1})	−24.14	1.8588
	R^2	0.2166	0.9283

highest R^2 values (1.00) for both pollutants in Table 1 and Fig. 5a, b. Whereas, the lowest R^2 values were observed for the power fraction and Elovich models, and there is no significant difference between both models for each pollutant, which represent the same values of 0.22 for PNP and 0.93 MB. The determination coefficient value of the pseudo-first-order model was ineffective in describing the adsorption process of the PNP, while the MB showed a relatively close value to unit (Table 2). The wellness of total PNP and MB sorption in the pseudo-second-order model suggests that the rate-limiting step in the sorption of PNP and MB onto the Ag°9 formula is the chemical sorption that is affected by the active sites of the adsorbent at ambient temperature (Mansee et al. 2023). This model considers that a quick reaction reaches equilibrium quickly in the beginning, followed by a slow reaction that can continue for extended periods. Adebayo et al. (2021) and Duman et al. (2020) studied the removal of MB by agar/κ-carrageenan hydrogel. Mansee et al. (2023) studied the removal of PNP using activated biochar. They found that pseudo-second order is the most suitable kinetic models for MB and PNP by agar/κ-carrageenan hydrogel and by activated biochar, respectively. q_e and q_t = the sorption capacities (mg g^{-1}) at equilibrium and contact time (t, min), respectively; k_1 (min^{-1}) = the constant extent of the pseudo-first; k_2 (g mg^{-1} min^{-1}) = the constant of pseudo-second-order sorption models and k_2 qe^2 (min) is the initial sorption rate mg g^{-1} min^{-1}; a = constant (mg g^{-1}); b = the rate constant (min^{-1}) of the power fraction model; α = the initial sorption rate (mg g^{-1} min^{-1}); β = constant of the Elovich model (g mg^{-1}).

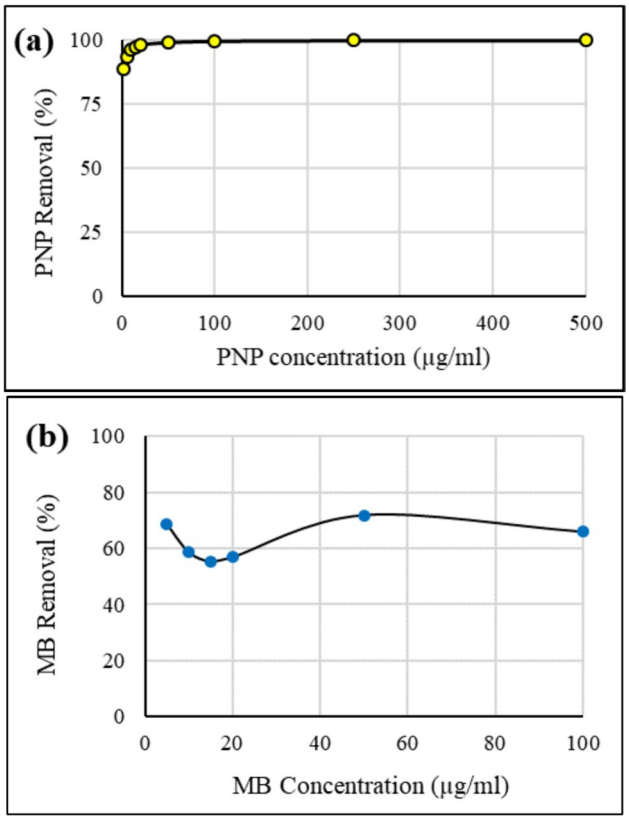

Fig. 6 Removal percentage of target pollutants by the Ag°9 formula after 5 min of incubation [**a** PNP concentrations = 2 to 500 µg ml^{-1}, Ag°9 dose = 60 µl ml^{-1}, contact time = 5 min., and **b** MB concentrations = 10 to 100 µg ml^{-1}, Ag°9 dose = 500 µl $ml.^{-1}$, contact time = 5 min]

Efficiency of Ag°9 for removing different concentrations of targeted pollutants

For PNP samples, the results showed increases in the sorbed amount of PNP per unit mass of Ag°9 with increasing the initial concentration of PNP (Fig. 6a). It may be due to the escalation in the mass driving force that permits more PNP molecules to pass from the solution to the surface of the adsorbent (Hamadeen et al. 2021). It can be concluded that 60 µL of Ag°9 formula was able to remove 99% of

500 µg ml^{-1} of PNP within the first 5 min. These results were confirmed by Devi and Ahmaruzzaman (2018) when they used green nanosilver for PNP reduction, and they found that 98.3% of the PNP was removed within 11 min. Also, Shimoga et al. (2020a, b) report that the silver nanoparticles have a beneficial and catalytic ability to degrade and redact PNP in the presence of aqueous sodium borohydride.

For MB samples, the results clarify that 500 µL Ag°9 was able to remove 68% of MB after 5 min of incubation (Fig. 6b). The same behavior was observed in the case of MB. This finding was agreement with Wang et al. (2018) when they studied the effect of initial MB concentration on the hydrogel beads of poly (vinyl alcohol) -sodium alginate-chitosan-montmorillonite removal efficiency. Therefore, it can be clarified that the present green nano formula (Ag°9) demonstrates superior performance in removing PNP more than those for MB.

The powerful Ag°9 formula for remediating PNP-MB mixture from artificially contaminated water

The efficiency of the current catalytic model was tested against a mixture of PNP-MB at different temperatures (5, 25, and 45 °C). When the reaction temperature increased to 45 °C, a slight increase in the removal percentage was observed (Fig. 7a). When the temperature decreased to 5 °C, the removal percentage decreased to 83 and 45% for PNP and MB, respectively. This finding was confirmed by Soni et al. (2018). When they studied the effect of temperature on MB removal, they concluded that as the temperature is increased, there is a decrease in the viscosity of the dye solution due to an increase in the rate of diffusion of the dye molecules across the external boundary layer. Figure 7b illustrates the UV spectra of the PNP-MB mixture before and after adding Ag°9. It was noticed two peaks at 400 and 665 nm, representing the presence of PNP and MB, respectively. Moreover, the optical densities of the PNP and MB were similar to their intensities in their single solution. At room temperature, a fast decline in those two peaks of intensity was achieved immediately by adding Ag°9, resulting in a 92% reduction in the case of PNP and a 55% reduction for MB after 5 min of treatment. Here, in this reaction, the Ag°9 shows outstanding activity, and reduction from either PNP or MB, respectively, was completed in 5 min. FTIR analysis was also used to study the effect of the interaction between the PNP-MB mixture and Ag°9 on the functional groups. The main functional groups of Ag°9 before and after use in mixture treatment of artificially contaminated water are illustrated in Fig. 7c. The FTIR spectrum of the Ag°9 formula before the adsorption shows different peaks at 3412.3, 2090, 1644.4, 1364.8, 1156.2, 1080.4, and 1023.5 cm^{-1}, while in the case of the Ag°9 formula after the adsorption process the peaks formed at 3412.3, 2085.2, 1639.7, 1151.5 and 1018.8 cm^{-1}. It was clarified that some of these functional groups shifted after the adsorption process, indicating a surface complex and electrostatic attraction with target pollutants. According to Mansee et al 2023, the formation of new absorption bands could be explained as follows: the change in the absorption intensity, and the wave number shift of the functional groups could result from the interaction of the sorbed component (PNP and MB) with the active sites of the sorbents (Ag°9). Also, Liu et al. (2022) reported that the rate of adsorption or removal may be related to different factors, such as the activated site's electrostatic attraction with charged molecular groups or complexation mechanism. Thus, in this investigation, the complexation mechanism explains the removal of pollutants through a mixture efficiency interaction.

A comparative account of PNP and MB adsorption by Ag° 9 with other sorbents

The present product Ag°9 as a sorbent material capacity was compared with different previous sorbents for removing PNP and MB (Fig. 8a, b) from contaminated water. The data reported in recent literature (2019–2023), (El Ouardi et al. 2019; Albukharia et al. 2019; Priyadarshini et al. 2021; Zhang et al. 2022; Erdem and Çetinkaya 2022; Mansee et al. 2023; Dao and Le Luu 2020; Bansal et al. 2021; Munir et al. 2020; Bayomie et al. 2020; Ullah et al. 2022; Zein et al. 2023) were compared on an equal basis using sorbent dose and the percentage of target pollutant removal with those of Ag°9. It is quite apparent that the green Ag°9 formula is able to achieve the same rate of removal by using trace doses ($2*10^{-6}$ and $1*10^{-5}$ g L^{-1} for removing PNP and MB, respectively). Thus, it is clear and obvious that the Ag°9 formula has shown promise and great potential as a green, low-cost sorbent for effective removal of *p*-nitrophenol and methylene blue from contaminated wastewater.

Conclusions

Green silver nanostructured materials are considered to be the most promising catalysts for $NaBH_4$-assisted PNP and MB reduction because of their unique advantages, such as the tunable shape and size of Ag NPs, high catalytic activity and stability, easy preparation, relatively low cost and toxicity, and environmental benignity. The present study's outcomes demonstrated the effectiveness of nanosilver green synthesis using *Hordeum vulgare* L. water extract in addition to its efficiency in remediating high concentrations of the PNP, MB, and PNP-MB mixtures of artificially contaminated water. To the best of our knowledge, this is one of the first reports of using *Hordeum vulgare* L. for the green synthesis of nanosilver without using any

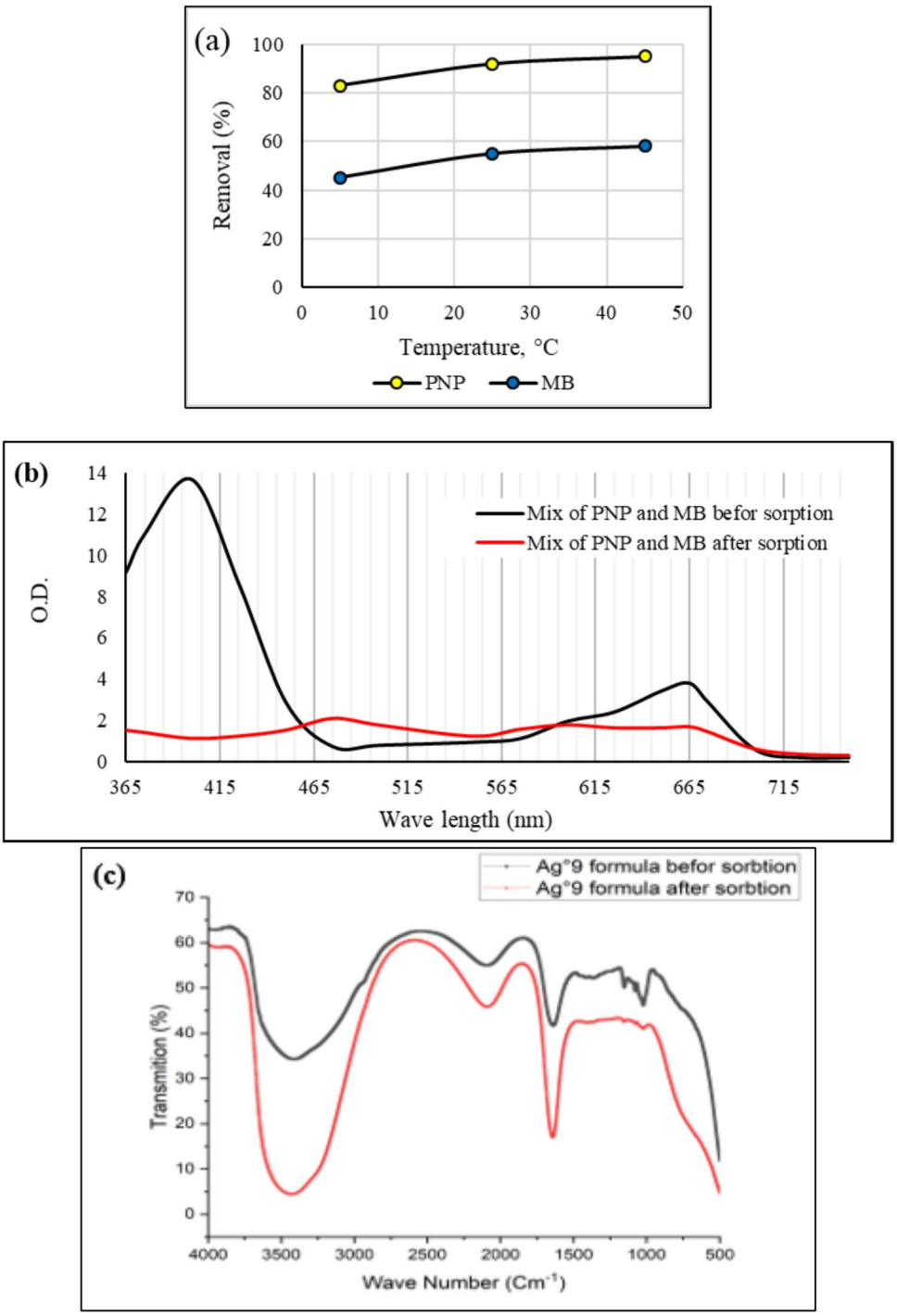

Fig. 7 UV–vis spectra of artificially contaminated water containing a mixture of PNP-MB before and after treatment with Ag°9 (**a**), effect of temperature on the removal percentage (**b**), and FTIR spectra of the Ag°9 formula before and after the remediation process (**c**) (PNP-MB = 100 µg ml^{-1}, Ag°9 dose = 500 µl ml^{-1}, and contact time = 5 min)

solvents. Moreover, their application for remediating artificially contaminated water with PNP and MB, either in a single or mixed case, is also shown as a new investigation. The spectroscopic measurements confirmed the presence of Ag° at a mean size of 27 nm. The Ag°9 formula achieved simultaneous and maximum elimination by using 60 µl/ml for PNP and 500 µl/ml for either MB or PNP-MB mixture during the first minute of incubation. Also, the current formula provided fast removal of target pollutants higher than 92 and 55% for PNP and MB in mixed cases within 5 min, respectively. The adsorption of the PNP and MB by the current formula was fitted to pseudo-second-order model. Therefore, this study provides an eco-friendly method for synthesizing Ag°, which can be used in the effluent treatment of different types of toxic organic pollutants.

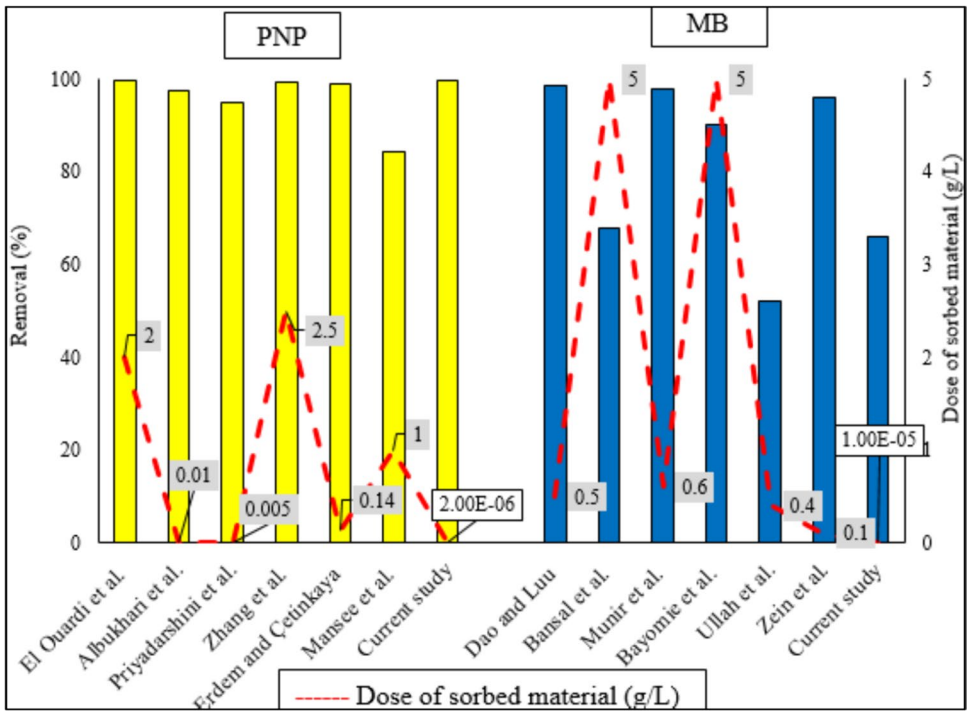

Fig. 8 survey of different sorbents potential for the removal of: **a** PNP and **b** MB from contaminated water

Author contributions The study conception and design were performed by Ayman H. Mansee. Material preparation, data collection and analysis were performed by Amal M. Ebrahim under supervision of Ayman H. Mansee and Essam A. Koreish. The first draft of the manuscript was written by Ayman H. Mansee, and all authors commented on previous versions of the manuscript. All authors read and approved the final manuscript.

Funding Open access funding provided by The Science, Technology & Innovation Funding Authority (STDF) in cooperation with The Egyptian Knowledge Bank (EKB).

Data availability The authors confirm that the data supporting the findings of this study are introduced and available within the manuscript.

Declarations

Conflict of interest The authors have no conflicts of interest to disclose, financially or otherwise.

Ethical approval The ethical standards were followed precisely during this study. Also, at every stage of the research, authors confirm:

No person or animal was exposed to any component of the materials used in the research, so that any harm would occur to him.
The authors did not use any live plants in this investigation.
Components or materials were not used in the research in a manner or concentration that would cause direct or indirect harm to the individuals carrying out the research or those in charge of the various measurement processes.
All the tools used in the research were dealt with in a scientific, healthy and accurate manner, which entails the safety of individuals and places in accordance with the governing local rules and laws.

Consent to participate Not applicable.

Consent to publish Not applicable.

References

Abada E, Mashraqi A, Modafer Y, Al Abboud MA, El-Shabasy A (2023) Review green synthesis of silver nanoparticles by using plant extracts and their antimicrobial activity. Saudi J Biol Sci, 103877

Abdelgawad DM, Marei AS, Mansee AH (2022) Managing the efficiencies of three different bacterial isolates for removing atrazine from wastewater. J Environ Sci Health B 57:948–959

Adebayo MA, Areo FI (2021) Removal of phenol and 4-nitrophenol from wastewater using a composite prepared from clay and Cocos nucifera shell: kinetic, equilibrium and thermodynamic studies. Resour Environ Sustain 3:100020

Albukharia SM, Ismailb M, Akhtara K, Ekram Y (2019) Catalytic reduction of nitrophenols and dyes using silver nanoparticles @ cellulose polymer paper for the resolution of waste water treatment challenges. Colloids Surf A 577:548–561

Attatsi IK, Nsiah F (2020) Application of silver nanoparticles toward Co (II) and Pb (II) ions contaminant removal in groundwater. Appl Water Sci 10:152. https://doi.org/10.1007/s13201-020-01240-0

Azeez L, Lateef A, Adebisi SA, Oyedeji AO (2018) Novel biosynthesized silver nanoparticles from cobweb as adsorbent for Rhodamine B: equilibrium isotherm, kinetic and thermodynamic studies. Appl Water Sci 8:1–12. https://doi.org/10.1007/s13201-018-0676-z

Bansal S, Pandey PK, Upadhayay S (2021) Methylene blue dye removal from wastewater using ailanthus excelsa roxb as adsorbent. Water Conserv Sci Eng 6:1–9. https://doi.org/10.1007/s41101-020-00097-3

Bayomie OS, Haitham Kandee H, Tamer Shoeib T, Hu Yang H, Youssef N, El-Sayed MH (2020) Novel approach for effective removal of methylene blue dye from water using fava bean peel Waste. Sci Rep 10:7824. https://doi.org/10.1038/s41598-020-64727-5

Behravan M, Panahi AH, Naghizadeh A, Ziaee M, Mahdavi R, Mirzapour A (2019) Facile green synthesis of silver nanoparticles using *Berberis vulgaris* leaf and root aqueous extract and its antibacterial activity. Int J Biol Macromol 124:148–154

Bilal M, Bagheri AR, Bhatt P, Chen S (2021) Environmental occurrence, toxicity concerns, and remediation of recalcitrant nitroaromatic compounds. J Environ Manage 291:112685

Chand K, Cao D, Fouad DE, Shah AH, Dayo AQ, Zhu K, Lakhan MN, Mehdi G, Dong S (2020) Green synthesis, characterization and photocatalytic application of silver nanoparticles synthesized by various plant extracts. Arab J Chem 13:8248–8261

Chartarrayawadee W, Charoensin P, Saenma J, Rin T, Khamai P, Nasomjai P, Too CO (2020) Green synthesis and stabilization of silver nanoparticles using Lysimachia foenum-graecum Hance extract and their antibacterial activity. Green Process Synth 9:107–118

Dao TM, Le Luu T (2020) Synthesis of activated carbon from macadamia nutshells activated by H_2SO_4 and K_2CO_3 for methylene blue removal in water. J Pre-Proof. https://doi.org/10.1016/j.biteb.2020.100583

Devi ThB, Ahmaruzzaman M (2018) Green synthesis of silver nanoparticles using Coccinia grandis fruit extract and its application toward the reduction of toxic nitro compounds. Indian J Chem Technol 25:475–841

Din MI, Tariq M, Hussain Z, Khalid R (2020) Single step green synthesis of nickel and nickel oxide nanoparticles from Hordeum vulgare for photocatalytic degradation of methylene blue dye. Inorg Nano-Metal Chem 50(4):292–297

Duh PD, Yen GC, Yen WJ, Chang LW (2001) Antioxidant effects of water extracts from barley (*Hordeum vulgare* L.) prepared under different roasting temperatures. J Agric Food Chem 49:1455–1463

Duman O, Polat TG, Diker CO, Tunç S (2020) Agar/κ-carrageenan composite hydrogel adsorbent for the removal of methylene blue from water. Int J Biol Macromol 160:823–835

El Ouardi M, Laabd M, Abou Oualid H, Younes Brahmi Y, Abaamrane A, Elouahli A, Addi AA, Laknifli A (2019) Efficient removal of p-nitrophenol from water using montmorillonite clay: insights into the adsorption mechanism, process optimization, and regeneration. Environ Sci Pollut Res 26:19615–19631. https://doi.org/10.1007/s11356-019-05219-6

Erdem HB, Çetinkaya S (2022) Facile insitu preparation of silver nanoparticles supported on petroleum asphaltene-derived porous carbon for efficient reduction of nitrophenols, 8(9)

Fouad DE, Zhang C, Mekuria TD, Bi C, Zaidi AA, Shah AH (2019) Effects of sono-assisted modified precipitation on the crystallinity, size, morphology, and catalytic applications of hematite (alpha-Fe2O3) nanoparticles: a comparative study. Ultrason Sonochem 59:104713. https://doi.org/10.1016/j.rinp.2019.01.005

Ganie AS, Bano S, Khan N, Sultana S, Rehman Z, Rahman MM, Khan MZ (2021) Nanoremediation technologies for sustainable remediation of contaminated environments: recent advances and challenges. Chemosphere 275:130065. https://doi.org/10.1016/j.chemosphere.2021.130065

Gopinath V, Priyadarshini S, Loke MF, Arunkumar J, Marsili E, Mubarakali D, Velusamy P, Vadivelu J (2017) Biogenic synthesis, characterization of antibacterial silver nanoparticles and its cell cytotoxicity. Arabian J Chem 10:1107–1117. https://doi.org/10.1016/j.arabjc.2015.11.011

Haldar AGM, Mahapatra DK, Dadure KM, Chaudhary RG (2022) Jordan journal of physics. Jordan J Phys 15(1):67–79

Hamadeen HM, Elkhatib EA, Badawy ME, Abdelgaleil SAM (2021) Green low cost nanomaterial produced from Moringa oleifera seed waste for enhanced removal of chlorpyrifos from wastewater: mechanism and sorption studies. J Environ Chem Eng 9:105376

Iravani S (2011) Green synthesis of metal nanoparticles using plants. Green Chem 13:2638

Kalpana D, Han JH, Park WS, Lee SM, Wahab R, Lee YS (2019) Green biosynthesis of silver nanoparticles using Torreya nucifera and their antibacterial activity. Arabian J Chem 12:1722–1732. https://doi.org/10.1016/j.arabjc.2014.08.016

Karki HP, Ojha DP, Joshi MK, Kim HJ (2018) Effective reduction of p-nitrophenol by silver nanoparticle loaded on magnetic Fe3O4/ATO nano-composite. Appl Surf Sci 435:599–608

Khan I, Saeed K, Zekker I, Zhang B, Hendi AH, Ahmad A, Khan I (2022) Review on methylene blue: its properties, uses, toxicity and photodegradation. Water 14(2):242

Khaturia S, Chahar M, Sachdeva H, Sangeeta MC (2020) A review: the uses of various nanoparticles in organic synthesis. J Nanomed Nanotech 11:543

Liao G, Chen J, Zeng W, Yu C, Yi C, Xu Z (2016) Facile preparation of uniform nanocomposite spheres with loading silver nanoparticles on polystyrene-methyl acrylic acid spheres for catalytic reduction of 4-nitrophenol. J Phys Chem C 120(45):25935–25944

Liao G, Gong Y, Zhong L, Fang J, Zhang L, Xu Z, Fang B (2019b) Unlocking the door to highly efficient Ag-based nanoparticles catalysts for NaBH 4-assisted nitrophenol reduction. Nano Res 12:2407–2436

Liao, G., Fang, J., Li, Q., Li, S., Xu, Z., & Fang, B. (2019a). Ag-Based nanocomposites: synthesis and applications in catalysis. *Nanoscale*, *11*(15), 7062–7096.)

Liu Y et al (2022) Efficient and rapid removal of typical phenolic compounds from water with biobased porous organic polymers. Ind Crops Prod 184:114971

Liu S, Deng F, Guo Y, Ouyang C, Yi S, Li C, Li Q (2023a) Silver nanocatalysts supported by multiple melanin carriers with a photothermal effect for reduction of methylene blue and 4-nitrophenol. ACS Appl Nano Mater 7(1):889–903

Liu S, Guo Y, Yi S, Yan S, Ouyang C, Deng F, Li Q (2023b) Facile synthesis of pure silicon zeolite-confined silver nanoparticles and their catalytic activity for the reduction of 4-nitrophenol and methylene blue. Sep Purif Technol 307:122727

Mansee AH, Abdelgawad DM, Marei AS (2020) Herbicide application history and different biostimulators effects on bacterial potency for atrazine bioremediation. Albaha Univ J Basic Appl Sci 4:15–21

Mansee AH, Abdelgawad DM, El-Gamal EH, Ebrahim AM, Saleh ME (2023) Influences of Mg-activation on sugarcane bagasse biochar characteristics and its PNP removing potentials from contaminated water. Sci Rep 13(1):19153

Mashkoor F, Nasar A (2020) Magsorbents: potential candidates in wastewater treatment technology—a review on the removal of methylene blue dye. J Magn Magn Mater 500:166408

Munir M, Nazar MF, Zafar MN, Zubair M, Ashfaq M, Hosseini-Bandegharaei A, Ahmad A (2020) Effective Adsorptive removal of methylene blue from water by didodecyldimethylammonium bromide-modified brown clay. ACS Omega 5(27):16711–16721

Mustafa I (2019) Methylene blue removal from water using H2SO4 crosslinked magnetic chitosan nanocomposite beads. Microchem J 144:397–402

Ouyang C, Liu S, Guo Y, Yi S, Li Q (2024) Silver nanoparticles decorated polydopamine-coated pure silica zeolite as an efficient nanocatalyst for organic pollutants removal. Appl Surf Sci 652:159281

Priyadarshini SS, Sethi S, Rout S, Mishra PM, Pradhan N (2021) Green synthesis of microalgal biomass-silver nanoparticle composite showing antimicrobial activity and heterogenous catalysis of nitrophenol reduction. Biomass Convers Biorefinery 13(9):7783–7795. https://doi.org/10.1007/s13399-021-01825-y

Rajegaonkar PS, Deshpande BA, More MS, Waghmare SS, Sangawe VV, Inamdar A, Adhapure NN (2018) Catalytic reduction of p-nitrophenol and methylene blue by microbiologically synthesized silver nanoparticles. Mater Sci Eng C 93:623–629

Saran S, Manjari G, Devipriya SP (2018) Synergistic eminently active catalytic and recyclable Ag, Cu and Ag-Cu alloy nanoparticles supported on TiO2 for sustainable and cleaner environmental applications: a phytogenic mediated synthesis. J Clean Prod 177:134–143

Sharma P, Pant S, Rai S, Yadav RB, Dave V (2017) Green synthesis of silver nanoparticle capped with allium cepa and their catalytic reduction of textile dyes: an ecofriendly approach. J Polym Environ 26(5):1795–1803. https://doi.org/10.1007/s10924-017-1081-7

Shimoga G, Palem RR, Lee S, Kim S (2020a) Catalytic degradability of p-nitrophenol using ecofriendly silver nanoparticles. Metals 10(12):1661. https://doi.org/10.3390/met10121661

Singh P, Mijakovic I (2024) Harnessing barley grains for green synthesis of gold and silver nanoparticles with antibacterial potential. Discover Nano 19(1):101

Singh V, Pant N, Sharma RK, Padalia D, Rawat PS, Goswami R, Deifalla AM (2023) Adsorption studies of Pb (II) and Cd (II) heavy metal ions from aqueous solutions using a magnetic biochar composite material. Separations 10(7):389

Soni S, Bajpai PK, Mittal J, Arora C (2020) Utilisation of cobalt doped Iron based MOF for enhanced removal and recovery of methylene blue dye from waste water. J Mol Liquids 314:113642

Ullah A, Muhammad Zahoor M, Din WU, Muhammad M, Khan FA, Sohail A, Ullah R, Ali EA, Murthy HCA (2022) Removal of methylene blue from aqueous solution using black tea wastes: used as efficient adsorbent. Adsorpt Sci Technol. https://doi.org/10.1155/2022/5713077

Wang W, Zhao Y, Bai H, Zhang T, Ibarra-Galvan V, Song S (2018) Methylene blue removal from water using the hydrogel beads of poly(vinyl alcohol)-sodium alginate-chitosan-montmorillonite. Carbohydr Polym 198:518–528. https://doi.org/10.1016/j.carbpol.2018.06.124

Zein R, Purnomo JS, Ramadhani P, Alif MF, Putri CN (2023) Enhancing sorption capacity of methylene blue dye using solid waste of lemongrass biosorbent by modification method. Arab J Chem 16(2):104480

Zhang Y, Shen Y (2017) Wastewater irrigation: past, present, and future. Wiley Interdiscip Rev WIREs Water. https://doi.org/10.1002/wat2.1234

Zhang J, Chen L, Zhang X (2022) Removal of p-nitrophenol by nano zero valent iron-cobalt and activated persulfate supported onto activated carbon. Water 14:1387. https://doi.org/10.3390/w14091387(2022)

Zhu H, Zhang C, Xie K, Li X, Liao G (2023) Photocatalytic degradation of organic pollutants over MoS2/Ag-ZnFe2O4 Z-scheme heterojunction: revealing the synergistic effects of exposed crystal facets, defect engineering, and Z-scheme mechanism. Chem Eng J 453:139775